Volume 9, Issue 6, 2019, 4581 - 4585 ISSN 2069-5837

Biointerface Research in Applied Chemistry

www.BiointerfaceResearch.com

https://doi.org/10.33263/BRIAC96.581585

Original Research Article Open Access Journal

Received: 12.09.2019 / Revised: 23.10.2019 / Accepted: 24.10.2019 / Published on-line: 26.10.2019

Spectroscopic and modeling analyses of bimolecular structure of corn silk

Gharieb W Ali [1,*], Wafa I. Abdel-Fattah [1], Hanan Elhaes [2], Medhat A. Ibrahim [3]

[1]Refractories, Ceramics and Building Materials Department; Biomaterials Group; National Research Centre, Egypt
[2]Physics Department, Faculty of Women for Arts, Science and Education, Ain Shams University, 11757, Cairo, Egypt
[3]Spectroscopy Department, National Research Centre, 33 El-Bohouth Str. 12622 Dokki, Giza, Egypt

*corresponding author e-mail address: ***medahmed6@yahoo.com*** |Scopus ID 8641587100

ABSTRACT

Corn silk (CS) is a protein/ cellulosic agricultural waste. Due to its documented beneficial medical applications; corn silk aqueous extract was greenly prepared. FTIR spectroscopic analyses are conducted for three fractions of CS, then a model is prepared to simulate CS molecular structure. Based on FTIR analyses, a model is described as composite of dehydrated alanine unit lignin unit and two cellulose units with metal oxides namely MgO and CuO. Some important descriptors were calculated with Quantitative structure–activity relationship QSAR calculations. Then quantum mechanical calculations were conducted. Molecular modeling data indicated the CS applicability for several biomedical applications due to its active sites proved by electrostatic potential. The results confirmed the suitability of CS as promising tool for many biological applications.

Keywords: *Corn silk; Molecular modeling; XPS, FESEM; Antioxidant activity.*

1. INTRODUCTION

Corn silk (Zea mays L.) is the residual of corn that is available in abundance worldwide [1]. Corn silk is a prestigious traditional Chinese medicine that has been widely used. It has a long history of application for therapeutic remedy and it was proved to be non-toxic [2]. It is rich in phenolic compounds known to significantly affect human health, such as anthocyanins, p-coumaric acid, vanillic acid, protocatechuic acid, derivatives of hesperidin and quercetin, and bound hydroxy cinnamic acid forms composed of p-coumaric and ferulic acid [3]. Moreover, it consists of various bioactive constituents which have a significant influence on human health. Corn silk has been reported to contain various chemicals, including proteins, vitamins, alkaloids, tannins and mineral salts, steroids, flavonoids and polysaccharides [4-8]. Corn silk bioactivities are widely reported in the literature, including antioxidant activities [9], anti-proliferative effects on human tumor necrosis factor (TNF) and lipopolysaccharide-induced cell adhesion [10], anti-diabetic activity on hyperglycemia rats [11], diuretic activity [12], anticoagulant activity [13] antifungal [14], anti-fatigue [15] and weight loss activities [16]. Antibiotic activity of flavone [17], immune enhancement by no starch polysaccharides, and anti-proliferative effects on human cancer cell lines are also reported [18]. CS fascinating biological activities are attributed to its polysaccharides contents and are the bases underlying publishing several articles dealing with the biological activities of the corn silk powder and extracts.

Molecular modeling is emerging as a powerful approach to study many systems and structures whereas experimental tools are limited, unavailable or even ethically not allowed. This paves the way toward the manipulation of biological systems by computational methods. Recently, Molecular modeling with different levels of theories is applied for describing bio-materials and other several classes of biological systems [19-24]. In this context, molecular modeling along with molecular spectroscopic methods are utilized together to understand several systems including CS [25-28]. However, researches combining molecular and physicochemical characterization of silk corn are seldom. Therefore, the present work aimed at studying the molecular structure with FTIR then to simulate the structure with QSAR and DFT molecular modeling

2. MATERIALS AND METHODS

2.1. Sampling.

Egyptian corn silk was collected, washed and left to dry at 37°C in an electric oven (Memert). The dried fibers were ground into powder using agitate mortar (Janke & Kunkel GmbH Co., Germany).

2.2. Characterization.

2.2.1. Fourier Infra-Red Spectroscopy (ATR-FTIR). FTIR spectra of the dried corn silk were collected at room temperature using the ATR unit attached with FTIR-Vertex 70 Bruker, Germany, in the range of 4000-400 cm^{-1}. The spectra were collected at three different points of the grinned corn silk sample as follows: solid (fibers), CS powder (intermediate size CS powder) and corn silk (very fine CS powder).

2.2.2. Calculations Details. The studied model molecule is subjected to energy minimization using Gaussian 09 sofcode [29]. The modeling program is implemented in personal computer. For total dipole moment, electrostatic potential the model is calculated with density functional theory at B3LYP together with LANL2DZ basis set [30-32].

Quantitative structure activity relationship (QSAR) was calculated for the same structure using SCIGRESS 3.0 software [33].

3. RESULTS

3.1. FTIR Spectroscopy.

Corn silk powder was subjected to FTIR spectroscopic study to elucidate its molecular structure. Corn silk powder was divided into three main parts namely the powder, the solid and fibers powder. The three spectra were collected in figure 1. The FTIR spectra of dried corn silk and corn silk fine powder are identical. The absorption band at 3282 cm^{-1} is due to the stretching vibration of −OH groups. While, the absorption band at 2923 cm^{-1} is corresponding to the inter- and intra-molecular interaction of the polysaccharide chains. The band at 1728 cm^{-1} is attributed to the elastic vibration of C=O groups (Amide I). On the other hand, the band at 1636 cm^{-1} can be attributed to the stretching of carboxylate group $(COO)^-$ and could also suggest the presence of N-H group proving corn silk protein. The bands at 1415 and 1375 cm^{-1} are attributed to C–H bending vibrations. Moreover, 1248 cm^{-1} band is ascribed to C-O stretching vibration. The intense 1031 cm^{-1} band is related to the sugar pyranose form. The FTIR spectrum of the unidentified solid component is quite different. The band at 3288 cm^{-1} is attributed to the stretching vibration of −OH groups. The bands at 2921 and 2856 cm^{-1} are corresponding to C-H asymmetric and symmetric stretching vibrations respectively. The Amide I elastic vibration band arises at 1715 cm^{-1}. The 1637 cm^{-1} and 1530 cm^{-1} bands are corresponding to stretching of carboxylate group $(COO)^-$ in asymmetric and stretching modes coupled with N-H bending vibration. The C–H bending vibrations are recorded at 1428-1381 cm^{-1}. A weak band at 1255 cm^{-1} can be related to C-O stretching vibration. The bands at 1151-1081 cm^{-1} are ascribed to ester and carboxylic acid. The pyranose form of sugar band is recorded at 1018 cm^{-1}. Finally, the bands at 871-840 cm^{-1} are related to anomeric vibration of β-glucosides [34-35].

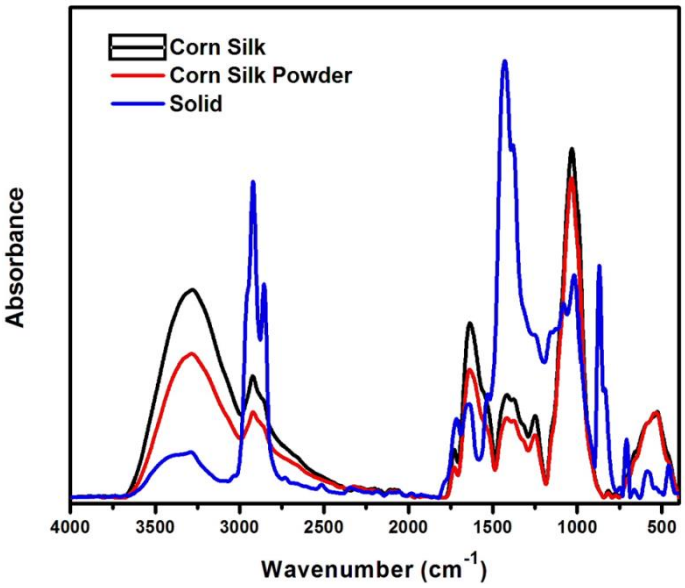

Figure 1. ATR-FTIR spectra for the studied corn silk: solid, powder and fibers grains.

3.2. Molecular Modeling Study.

Based on the molecular structure of the corn silk, a model could be simulated with DFT. The spectra suggested that CS is a composite of lignin unit of two cellulose units with metal oxides namely MgO and CuO. The structure contains alanine unit as an indicator for the protein existence and is hydrated with two water molecules linked electrostatically with the alanine two active sites. In this context, lignin and cellulose are linked throughout their O-linkage. Finally, the two metal oxides are linked via weak interactions through the oxygen of the O-linkage for the two cellulose units.

3.2.1. Quantum Mechanical Calculations. B3LYP/LANL2DZ results for the CS studied structure is indicated in table 1 presenting the total dipole moment and HOMO/LUMO band gap energy.

Table 1. Total dipole moment TDM and HOMO/LUMO band gap energy as eV which is calculated at B3LYP/LANL2DZ level of theory.

Total dipole moment TDM	ΔE
10.6165	1.6662

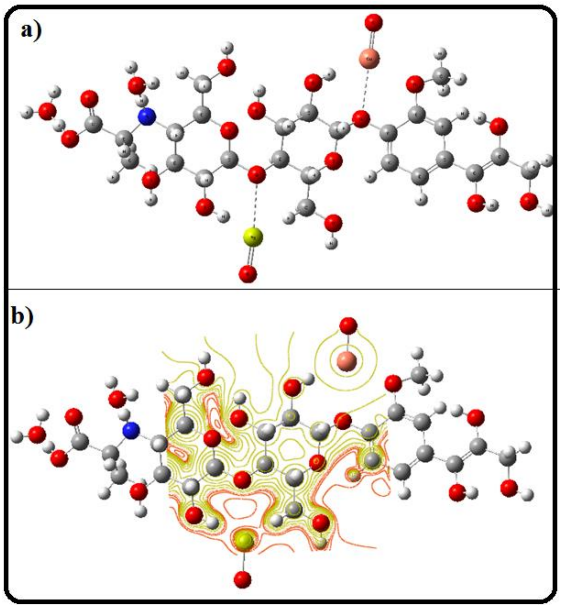

Figure 2. a) Model molecule for CS which consists of two cellulose units, one lignin unit, one alanine unit, MgO, CuO and two water molecules, b) Molecular electrostatic potential calculated at B3LYP/LANL2DZ level of theory.

The contour of molecular ESP describing the corn silk surface was achieved through mapping the sites for the electrophilic and nucleophilic attacks. This contour describes the charge distributions for the studied structure throughout colors [36]. Mapping the colors indicates the site, each color represents a certain charge so that, from negative to positive, the colors are going to change from red to blue. The negativity is following color scheme according to the following color order red< orange < yellow < green < blue [37, 38]. The molecular electrostatic potential is calculated at the same level of theory (Fig.2). Red colors are surrounding the oxygen of the amino acid carboxylic group and the CuO. The water molecules oxygen is represented by red color contour (Fig.2 a). The active sites in CS are not for amide group but for sites close to the polar water molecules and to CuO.

These results could be further confirmed with the HOMO/LUMO band gap energy as indicated in figure 2 b).

The total dipole moment was calculated as 10.6165 Debye while the HOMO/LUMO band gap was 1.6662 eV.

The HOMO/LUMO is localized around the CuO, which could be a confirmation that it is one of the active sites in the CS studied model structure.

Upon increasing the total dipole moment with decreasing the band gap indicates the reactivity of the studied structure [39-40]. Moreover, ESP, TDM and HOMO/LUMO are collectively indicating the ability of the studied structure for further interacting with its surroundings. Therefore, the corn silk model contains several active sites and its reactivity is dedicated to various biomedical applications (Figure 3).

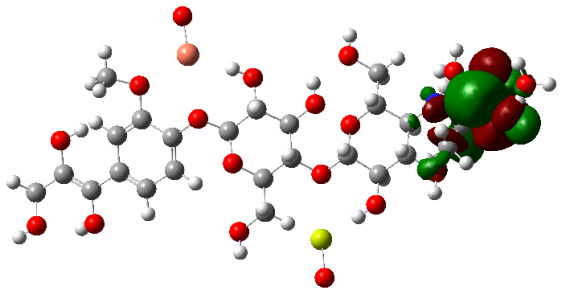

Figure 3. HOMO/LUMO band gap energy which is calculated at B3LYP/LANL2DZ level of theory.

3.2.2. QSAR Calculations. Other variations for the studied model could be achieved with the descriptors of the quantitative structure activity relationship. Table 2 presents the calculated physical and electronic properties of corn silk, total energy (E), and QSAR properties; ionization potential (IP), log P, molar refractivity, polarizability, surface area (A) and volume (V) calculated at PM6 level. The proposed structure is optimized using semi-empirical quantum mechanical calculations at PM6 level. The optimization process results in some physical and electronic properties as charge, total energy (E). The optimization calculation process shows that the optimized structure possesses quite high stabilization where its total energy is -266698.162 kcal/mol. Further, the QSAR parameters are calculated at the same PM6 level. They are conducted to investigate the biological activity of the proposed compound. QSAR properties such as ionization potential (IP), log P, molar refractivity, polarizability, surface area and volume were calculated (Table 2). Regarding the ionization potential, the energy required to remove an electron from the structure to an infinite distance is -8.936eV. For the log P property referring to the hydrophilic nature of the structure where positive values indicate hydrophobic structures while negative ones reflect the hydrophilic compounds. It is obvious from the calculated log P parameter that the structure owns hydrophilic nature. This is attributed to several hydroxyl groups existence in its structure. Molar refractivity property is calculated to be 143.448. Furthermore, surface area and volume parameters are calculated to be 607.52 A2 and 535.12 A3 respectively. Polarizability property that depends on both the surface area and volume was calculated. It reflects how ease the structure can be polarized.

Table 2. QSAR descriptors for the studied structure at PM6 semispherical level of theory, the calculated parameters including total energy (E), and QSAR properties; ionization potential (IP), log P, molar refractivity, polarizability, surface area (A) and volume (V).

E (kcal/mol)	IP (eV)	log P	Molar refractivity	Polarizability	A (A^2)	V (A^3)
-266698.16	-8.94	-2.176	143.45	48.88	607.52	535.12

4. CONCLUSIONS

The CS biological reactivity is attributed to several active functional groups as hydroxyl groups in both lignin and cellulose units in addition to the amide one in the introduced alanine amino acid. Furthermore, the existing metal oxides and the two water molecules are sharing also in the reactivity of the proposed structure. Correlating the quantum mechanical results with QSAR results, the reactivity of the studied corn silk model molecule can be observed. The above mentioned structure is responsible for the promising biological activity proposing the CS reliable matrix for several biological applications.

5. REFERENCES

1. Yang, J.; Li, X.; Xue, Y.; Wang, N.; Liu, W. Anti-hepatoma activity and mechanism of corn silk polysaccharides in H22 tumor-bearing mice. *Int. J. Biol. Macromol.* **2014**, *64*, 276–280, https://doi.org/10.1016/j.ijbiomac.2013.11.033.
2. Wang, C.; Zhang, T.; Liu, J.; Lu, S.; Zhang, C.; Wang, E.; Wang, Z.; Zhang, Y.; Liu, J. Subchronic toxicity study of corn silk with rats. *J. Ethnopharmacol.* **2011**, *137*, 36–43, https://doi.org/10.1016/j.jep.2011.03.021.
3. Pooyan, M.;, Ghareib, W.; Francesca, D.; Wafa ,I. ; Assunta,B.; Biosynthesis and characterization of antibacterial thermosensitive hydrogels based on corn silk extract, hyaluronic acid and nanosilver for potential wound healing, *Carbohydr. Polym.* **2019**, 223, 115023. https://doi.org/10.1016/j.carbpol.2019.115023.
4. Fauguela, C. M.; Campos ,V., A.; Iglesiasa , J.; Fernandeza , M.; Farronia , A. ; Andreob, C. S.; Preselloa D. A.; Volatile compounds released by maize grains and silks in response to infection by Fusarium verticillioides and its association with pathogen resistance, *Plant Pathol.* **2017**, 66, 1128–1138. https://doi.org/10.1111/ppa.12663.
5. Maksimovic, Z.A.; Kovacevic, N. Preliminary assay on the antioxidative activity of *Maydis stigma* extracts. *Fitoterapia* **2003**, *74*, 144–147, https://doi.org/10.1016/S0367-326X(02)00311-8.
6. Qingwen, G.; Leilei, X.; Yue, C.; Qiqi, M.; Ramesh, K.; Zihan, X.; Xudong, G.; Haixia, C.; Structural characterization of corn silk polysaccharides and its effect in H2O2 induced oxidative damage in L6 skeletal muscle cells. *Carbohydrate Polym.*, **2019**, 208, 161-167. https://doi.org/10.1016/j.carbpol.2018.12.049
7. Ren, S.; Ding, X.; Study on determination methods of flavonoids from corn silk. Shipin Kexue. 2004, 25, 139–142. Peng, L.; bomir; L.; Barbora, L.;Sergii, K.; Physico-chemical study of flavonoids from different matureness corn silk material, *Potravinarstvo* , **2018**, 12, 347-354. DOI: https://doi.org/10.5219/869.
8. Wang, K.J.; Zhao, J. L.; Corn silk (Zea mays L.), a source of natural antioxidants with α-amylase, α-glucosidase, advanced glycation and diabetic nephropathy inhibitory activities, *Biomed.*

Pharmacother. **2019,** 110, 510-517. http://dx.doi.org/10.1016/j.biopha.2018.11.126.

9. Yuxiang, P.; Cong, W.; Zhongqin, C.; Weiwei, L.; Guoqi, Y.; Haixia, C.; Physicochemical properties and antidiabetic effects of a polysaccharide from corn silk in high-fat diet and streptozotocin-induced diabetic mice, *Carbohydr. Polym.* **2017**, 164, 370-378. http://dx.doi.org/10.1016/j.ijbiomac.2013.11.033.

10. Habtemariam, S. Extract of corn silk (stigma of Zea mays) inhibits the tumour necrosis factor-alpha- and bacterial lipopolysaccharide-induced cell adhesion and ICAM-1 expression. *Planta Med.* **1998**, *64*, 314-8, https://doi.org/10.1055/s-2006-957441.

11. Zhao, W.; Yin, Y.; Yu, Z.; Liu, J.; Chen, F. Comparison of anti-diabetic effects of polysaccharides from corn silk on normal and hyperglycemia rats. *Int. J .Biol. Macromol.* **2012**, *50*, 1133-7, https://doi.org/10.1016/j.ijbiomac.2012.02.004.

12. Velazquez, D.V.; Xavier, H.S.; Batista, J.E.; Castro-Chaves, C. Zea mays L. extracts modify glomerular function and potassium urinary excretion in conscious rats. *Phytomedicine* **2005**, *12*, 363-369, https://doi.org/10.1016/j.phymed.2003.12.010.

13. Kyung, A.K.; Choi, S.K.; Choi, S.H. Corn silk induces nitricoxide synthase in murinemacrophages. *Experimental and Molecular Medicine* **2004**, *36*, 545-550, https://doi.org/10.1038/emm.2004.69.

14. Miller, S.S.; Reid, L.M.; Harris, L.J. Colonization of maize silks by Fusarium graminearum, the causative organism of gibberella ear rot. *Canadian Journal of Botany* **2007**, *85*, 369-376, https://doi.org/10.1139/B07-027.

15. Jiandong, W.; Miao, Y.; Zaigui, W.; Extraction, Purification and Anti-Hyperlipidemic Activities of Total Flavonoids from Corn Silk, *Pakistan J. Zool.* **2017,** 49, 2173-2179, http://dx.doi.org/10.17582/journal.pjz/2017.49.6.2173.

16. Maksimovic, Z.; Dobric, S.; Kovacevic, N.; Milovanovic, Z. Diuretic activity of Maydis stigma extract in rats. *Pharmazie* **2004**, *59*, 967-971. https://doi.org/10.1004/15638089.

17. Slađana, Ž.; Marijana, J.; Zorica, B.; Jelena, V.; Vuk, M.; Antioxidant activity, phenolic profile, chlorophyll and mineral matter content of corn silk (Zea mays L): Comparison with medicinal herbs. *J. Cereal Sci.* **2016**, 69, 363-370. https://doi.org/10.1016/j.jcs.2016.05.003.

18. Hao, G.; Hong, G.; Wenqin, Y.; Han, L.; Huiling, H.; Xue, C.; Zhenyan, L.; Chuangang, Z.; Yuchao, L.; Jicheng, L. Pro-apoptotic and anti-proliferative effects of corn silk extract on human colon cancer cell lines. *Oncol Lett.* **2017**, *13*, 973-978, https://doi.org/10.3892/ol.2016.5460.

19. Kirstin, A.; Marco, B.N.; Andriy, Z.R. The 2019 materials by design roadmap: Introduction . J. Phys. D: Appl. Phys. 2018, 52, 013001.

20.

21. Eugene, S.K.; Eduardo, V.L. Density functional theory: Foundations reviewed. *Physics Reports* **2014**, *544*, 123-239, https://doi.org/10.1016/j.physrep.2014.06.002.

22. Badry, R.;, Omar, A.; Mohammed, H.; Mohamed, D.A.A.; Elhaes, H.; Refaat, A.; Ibrahim, M. Effect of Alkaline Elements on the Structure and Electronic properties of Glycine. *Biointerface Research in Applied Chemistry* **2018**, *8*, 3682-3687.

23. Mahmoud, A.Z.; Osman, O.; Elhaes, H.; Ferretti, M.; Fakhry, A.; Ibrahim, M. Computational Analyses for the Interaction Between Aspartic Acid and Iron. *J. Comput. Theor. Nanosci.* **2018**, *15*,470–473, https://doi.org/10.1166/jctn.2018.7113.

24. Dheivamalar, S.; Silambarasan, V. DFT simulations and vibrational analysis of FTIR and FT-Raman spectra of 2-amino-4-methyl benzonitrile. *Spectrochimica Acta Part A* **2012**, *96*, 480-484, https://doi.org/10.1016/j.saa.2012.05.008.

25. Aydin, M. DFT and Raman spectroscopy of porphyrin derivatives: Tetraphenylporphine (TPP). *Vibrational Spectroscopy* **2013**, *68*, 141-152, https://doi.org/10.1016/j.vibspec.2013.06.005.

26. Alam, M.J.; Khan, A.U.; Alam, M.; Ahmad, S. Spectroscopic (FTIR, FT-Raman, 1H NMR and UV–Vis) and DFT/TD-DFT studies on cholesteno [4,6-b,c]-2′,5′-dihydro-1′,5′-benzothiazepine. *Journal of Molecular Structure* **2019**, *1178*, 570-582, https://doi.org/10.1016/j.molstruc.2018.10.063.

27. Galal, A.M.F.; Shalaby, E.M.; Abouelsayed, A.; Ibrahim, M.A.; Al-Ashkar, E.; Hanna, A.G. Structure and absolute configuration of some 5-Chloro-2-methoxy-N-phenylbenzamide derivatives. *Spectrochim. Acta A.* **2018**, *188*,213-221, https://doi.org/10.1016/j.saa.2017.06.068.

28. Abdel-Gawad, F.K.; Osman, O.; Bassem, S.M.; Nassar, H.F.; Temraz, T.A.; Elhaes, H.; Ibrahim, M. Spectroscopic Analyses and Genotoxcity of Dioxins in the Aquatic Environment of Alexandria. *Marine Pollution Bulletin.* **2018,** *127*, 618-625, https://doi.org/10.1016/j.marpolbul.2017.12.056.

29. Alaaeldin, M.F.G.; Atta, D.; Abouelsayed, A.; Ibrahim, M.A.; Hanna, A.G. Configuration and Molecular Structure of 5-Chloro-N-(4-sulfamoylbenzyl) Salicylamide Derivatives. *Spectrochim. Acta A.* **2019**, *214*, 476-486, https://doi.org/10.1016/j.saa.2019.02.070.

30. Gaussian 09, Revision C.01, Frisch, M.J.; Trucks, G.W.; Schlegel, H.B.; Scuseri, G. E. M.A.; Cheeseman, J.R.; Scalmani, G.; Barone, V.; Mennucci, P. B. G. A., Nakatsuji, H.; Caricato, M.; Li, X. HratchianP; Izmaylov, A.F.; Bloino, J.; Zheng, G.; Sonnenberg, J.L.; Hada, M.; Ehara, M.; Toyota, K.; Fukuda, R.; Hasegawa, J.; Ishida, M.; Nakajima ,T . ; Honda, Y.; Kitao, O.; Nakai, H.; Vreven, T.; Montgomery, J.A; Peralta, J.E.; Ogliaro, F.; Bearpark, M.; Heyd , J.J.; Kudin, K.N.; Staroverov, V.N.; Keith, T.; Kobayashi, R., Normand .J.; Raghavachari, K.; Rendell, A.; Burant, J.C.; Iyengar, S.S.; Tomasi, J.; Cossi, M.; Rega, N.; Millam, J.M.; Klene, M.; Knox, J.E.; Cross, J.B.; Bakken, V.; Adamo, C.; Jaramillo, J.; Gomperts, R.; Stratmann, R.E.; Yazyev, O.; Austin, A.J.; Cammi, R.; Pomelli, C.; Ochterski, J.W.; Martin, R.L.; Morokuma, K.; Zakrzewski, V.G.; Voth, G.A.; Salvador, P.; Dannenberg, J.J.; Dapprich, S.; Daniels, A.D.; Farkas, O.; Foresman, J.B.; Ortiz, J.V.; Cioslowski, J.; Fox, D.J. Gaussian, Inc., Wallingford CT **2010**.

31. Becke, A.D. Density functional thermochemistry. III. The role of exact exchange. *Chem. Phys.* **1993**, *98*, 5648-5652, https://doi.org/10.1063/1.464913.

32. Lee, C.; Yang, W.; Parr, R.G. Development of the Colle-Salvetti correlation-energy formula into a functional of the electron density. *Phys. Rev. B.* **1988**, *37*, 785-789, https://doi.org/10.1103/PhysRevB.37.785.

33. Miehlich, B.; Savin, A.; Stoll, H.; Preuss, H. Results obtained with the correlation energy density functionals of becke and Lee, Yang and Parr. *Chem. Phys. Lett.* **1989**, *157*, 200-206, https://doi.org/10.1016/0009-2614(89)87234-3.

34. Summers, K.L.; Mahrok, A.K.; Dryden, M.D.; Stillman, M.J. Structural properties of metal-free apometallothioneins. *Biochem Biophys Res Commun.* **2012**, *425*, 485-492, https://doi.org/10.1016/j.bbrc.2012.07.141.

35. Qingwen, G.; Qiqi, Ma.; Zihan, X.;, Xudong, G.; Haixia, C. Studies on the binding characteristics of three polysaccharides with different molecular weight and flavonoids from corn silk (Maydis stigma). *Carbohydr Polym.*, **2018**, *198*, 581-588, https://doi.org/10.1016/j.carbpol.2018.06.120.
36. Atefeh, A.; Majid, M.; Mahnaz, M. Synthesis of applicable hydrogel corn silk/ZnO nanocomposites on polyester fabric with antimicrobial properties and low cytotoxicity. *Int. J. Biol. Macromol*. **2019**, *123*, 1079-1090, https://doi.org/10.1016/j.ijbiomac.2018.11.093.
37. Politzer, P.; Laurence, P.R.; Jayasuriya, K. Molecular electrostatic potentials: an effective tool for the elucidation of biochemical phenomena. *Environ. Health Persp.* **1985**, *61*, 191-202, https://doi.org/10.1289/ehp.8561191.
38. Politzer, P.; Murray, J.S. Molecular Electrostatic Potentials: Concepts and Applications. *J. Theor. Comput. Chem*. **1996**, *3*, 649.
39. Şahin, Z.S.; Şenöz, H.I.; Tezcan, H.; Büyükgüngör, O. Synthesis, spectral analysis, structural elucidation and quantum chemical studies of (E)-methyl-4-[(2-phenylhydrazono)methyl]benzoate. *Spectrochim. Acta A* **2015**, *143*, 91-100, https://doi.org/10.1016/j.saa.2015.02.032.
40. Ibrahim, M.; El-Haes, H. Computational Spectroscopic Study of Copper, Cadmium, Lead and Zinc Interactions in the Environment. *Int. J. Environ. Pollut.* **2005**, *23*, 417-424, https://dx.doi.org/10.1504/IJEP.2005.007604.
41. Ibrahim, M.; Mahmoud, A.A. Computational Notes on the Reactivity of some Functional Groups. *J. Comput. Theor. Nanosci*. **2009**, *6*, 1523-1526, http://dx.doi.org/10.1166/jctn.2009.1205.